Lattice sites of implanted Fe in Si

U. Wahl,* J. G. Correia, and E. Rita
Instituto Tecnológico e Nuclear, Estrada Nacional 10, 2686-953 Sacavém, Portugal
and Centro de Física Nuclear da Universidade de Lisboa, Avenida Professor Gama Pinto 2, 1649-003 Lisboa, Portugal

J. P. Araújo
Departamento de Física, Universidade do Porto, Rua do Campo Alegre 687, 4169-007 Porto, Portugal

J. C. Soares
Centro de Física Nuclear da Universidade de Lisboa, Avenida Professor Gama Pinto 2, 1649-003 Lisboa, Portugal

The ISOLDE Collaboration
CERN-PH, 1211 Genève 23, Switzerland
(Received 21 March 2005; published 14 July 2005)

The angular distribution of β^- particles emitted by the radioactive isotope ^{59}Fe was monitored following implantation into Si single crystals at fluences from 1.4×10^{12} cm^{-2} to 1×10^{14} cm^{-2}. We identified Fe on three distinct sites: ideal substitutional, displaced substitutional and displaced tetrahedral interstitial. Whereas displaced substitutional Fe was dominating for annealing temperatures below 500 °C, annealing between 500–700 °C caused the majority of Fe to occupy displaced tetrahedral interstitial sites. Ideal substitutional positions were increasingly populated following annealing at 800 °C and above. A comparison of the emission channeling results to Mössbauer and electron paramagnetic resonance experiments is given.

DOI: 10.1103/PhysRevB.72.014115 PACS number(s): 61.72.−y, 61.72.Tt, 61.72.Yx

I. INTRODUCTION

Due to the richness of the electrical and optical phenomena associated with Fe in silicon, it represents one of the most fascinating impurities and has been studied for decades, as is reviewed in Refs. 1–3. The importance of understanding the properties of Fe in Si is further underlined by its role in Si processing, where it acts, together with other transition metals such as Cu, Ni or Co, as one of the most dangerous contaminants. As a consequence, detailed and costly gettering schemes have to be applied in order to remove the transition metals from the active region of devices.[1–4] Among the various gettering schemes, defects resulting from ion implantation have proven to act as effective gettering centers,[5–8] giving a good motivation to study the behavior of Fe also in the presence of implantation damage.

With respect to possible lattice sites of Fe in Si, the existence of interstitial Fe in sites of tetrahedral T_d symmetry has been generally accepted since the electron paramagnetic resonance (EPR) work of Ludwig and Woodbury.[9] Based on these EPR observations most theoretical approaches focused on iron on ideal tetrahedral interstitial sites (see Refs. 10–14 and references therein), but, with the exception of Fe-acceptor pairs,[15] never in a configuration of symmetry lower than T_d.

Some theoretical works also considered substitutional Fe,[10,13,16,17] however, only in an ideal substitutional configuration. The existence of any form of substitutional Fe has been the subject of much speculation and lacks direct experimental confirmation. By means of EPR, the so-called *NL*19 center of trigonal C_{3v} symmetry was found in Fe-doped electron-irradiated Si.[18,19] As a microscopic model for this center an "interstitial Fe atom paired with a Si vacancy" was proposed, resulting in Fe near a substitutional site from which it is shifted along a ⟨111⟩ direction.

The most convincing evidence for substitutional Fe in Si so far comes from Mössbauer experiments. The general picture which has emerged from these studies is that Fe in Si produces four characteristic Mössbauer signals: (a) a quadrupole-split doublet with $\delta=+0.20-0.33$ mm/s and $E_Q=0.83-1.0$ mm/s (at 300 K) which results from Fe in a damaged environment[17,20–25] and is sometimes also termed the "amorphous" site;[26] (b) a singlet of isomer shift $\delta=+0.76-0.86$ mm/s (at 300 K) which is without doubt due to interstitial Fe;[17,20–27] (c) a second singlet with $\delta=-(0.08-0.03)$ mm/s (extrapolated to 0 K) which originates from substitutional Fe;[17,20–27] (d) a second doublet with $\delta=+0.44-0.51$ mm/s and $E_Q=0.6$ mm/s (extrapolated to 0 K), which has been termed the "unknown"[21] or "new" line[22,24] and is attributed to Fe on interstitial sites paired with a vacancy.

However, with respect to direct lattice location methods, not much is actually known on Fe in Si. This is due to the fact that most structural techniques lack sensitivity at lower Fe concentrations and at higher concentrations Fe forms silicides. Bunker[28] studied Si implanted with 10^{16} cm^{-2} of Fe at 100 keV and annealed between 600 °C and 800 °C, using the method of extended x-ray absorption fine structure (EXAFS). It was concluded that the EXAFS results are consistent with Fe being located at a distorted interstitial site. Vartanyantz *et al.*[29] investigated Si implanted with 5×10^{15} cm^{-2} of Fe at 80 keV and annealed at 750 °C using Rutherford backscattering spectroscopy and channeling (RBS/C) They found that the RBS signal from Fe was reduced by 30% for ⟨111⟩ channeling incidence, from which they concluded that 30% of Fe would be located on substi-

TABLE I. Characteristics of the investigated Si samples. FZ means float zone and CZ Czochralski-grown material. All *p*-type samples were B-doped and all *n*-type samples P-doped.

Sample No.	Type	Resistivity (Ω cm)	Growth method	Surface	Implanted fluence (cm^{-2})
1	*P*	10 000	FZ	$\langle 111 \rangle$	1.4×10^{12}
2	*P*	10–20	FZ	$\langle 100 \rangle$	5.3×10^{12}
3	*P*	10 000	FZ	$\langle 111 \rangle$	5.4×10^{12}
4	*P*	12–16	epi[a]	$\langle 100 \rangle$	1.2×10^{13}
5	*P*	10–20	FZ	$\langle 100 \rangle$	1.6×10^{13}
6	*P*	10 000	FZ	$\langle 111 \rangle$	2.0×10^{13}
7	*P*	10–20	FZ	$\langle 100 \rangle$	4.8×10^{13}
8	*P*	10 000	FZ	$\langle 111 \rangle$	1.0×10^{14}
9	*N*	700–1300	FZ	$\langle 111 \rangle$	4.0×10^{12}
10	*N*	7.3–12	CZ[b]	$\langle 111 \rangle$	4.9×10^{12}
11	*N*	0.03	CZ	$\langle 100 \rangle$	8.0×10^{12}
12	*N*	700–1300	FZ	$\langle 111 \rangle$	8.5×10^{12}
13	*N*	7.3–12	CZ[b]	$\langle 111 \rangle$	1.0×10^{13}
14	*N*	700–1300	FZ	$\langle 111 \rangle$	4.0×10^{13}

[a]The thickness of the epitaxial layer of the epi-Si sample #4 was 6–7 μm on a 0.01–0.02 Ω cm p^+-substrate.
[b]The oxygen concentration of samples #10 and #13 was characterized as $6.5–6.7 \times 10^{17}$ cm^{-3} by the manufacturer.

tutional sites. However, this conclusion is ambiguous since reductions in the backscattering yield for $\langle 111 \rangle$ channeling may result not only from substitutional but also from a large variety of interstitial sites in Si.

We present here direct lattice location experiments of implanted Fe in Si. We were able to clearly identify Fe on at least 3 distinct sites: ideal substitutional sites (*S*), displaced substitutional sites (near-*S*), and displaced tetrahedral interstitial sites (near-*T*). We used the β^- emission channeling technique,[30] which makes use of the fact that charged particles emitted from radioactive isotopes in single crystals experience channeling or blocking effects along low-index crystal directions. This leads to an anisotropic emission yield from the crystal surface which depends in a characteristic way on the lattice sites occupied by the emitter atoms.

II. EXPERIMENT

In order to dope with long-lived ^{59}Fe ($t_{1/2}$=44.6 *d*) we implanted the precursor isotope ^{59}Mn ($t_{1/2}$=4.6 *s*) at the ISOLDE on-line isotope separator facility at CERN. ISOLDE provides clean, mass-separated beams of radioactive Mn isotopes, which are produced by means of 1.4-GeV proton-induced nuclear fission from UC_2 targets and chemically selective laser ion sources.[31] During the β^- decay of the ^{59}Mn nucleus the resulting ^{59}Fe atom receives a recoil around 200 eV, which assures that it is reimplanted and hence that its lattice position is not influenced by the previous site of ^{59}Mn.

Fourteen Si single crystals were investigated. Table I gives their doping type, resistivity, growth method, surface orientation, and the implanted fluences. All implantations were done at room temperature under an angle of 7° to the surface normal in order to avoid channeled implantation and produce a well-defined depth profile. The depth profiles for these implantation conditions, as estimated by means of the SRIM 2003 (Ref. 32) or MARLOWE (Ref. 33) codes, are approximately Gaussian, centered at 532 Å with a straggling of 192 Å and peak concentrations of 2.0×10^5 $(atoms/cm^3)/(atoms/cm^2)$.

Following the implantation the crystals were mounted on a goniometer using sample holders entirely made of Ta and Mo. Annealing up to 900 °C in steps of 100 K (10 min) was done *in situ* under vacuum better than 10^{-6} mbar. While the setpoint temperature was reached after 1–2 min, the cool down to room temperature lasted up to 30 min since the samples could not be quenched under vacuum. After each annealing step, the β^- emission yield in the energy window 50–461 keV was measured at room temperature using the position-sensitive detector systems described in Refs. 34 and 35 as a function of angle from $\langle 100 \rangle$, $\langle 111 \rangle$, $\langle 110 \rangle$, and $\langle 211 \rangle$ directions.

III. RESULTS

Let us first present the experimental results for sample #8 obtained after annealing at the three characteristic temperatures of 300 °C, 600 °C, and 800 °C. Following annealing at 300 °C [Figs. 1(a)–1(d)], the fact that channeling is observed along all major axes, $\langle 111 \rangle$, $\langle 100 \rangle$, $\langle 110 \rangle$, and $\langle 211 \rangle$ and the closest-packed planes, {110}, {100}, and {111}, is clear evidence that the majority of Fe atoms are located on or near substitutional sites. Following 600 °C annealing the overall shape of the $\langle 111 \rangle$ and $\langle 100 \rangle$ patterns is almost un-

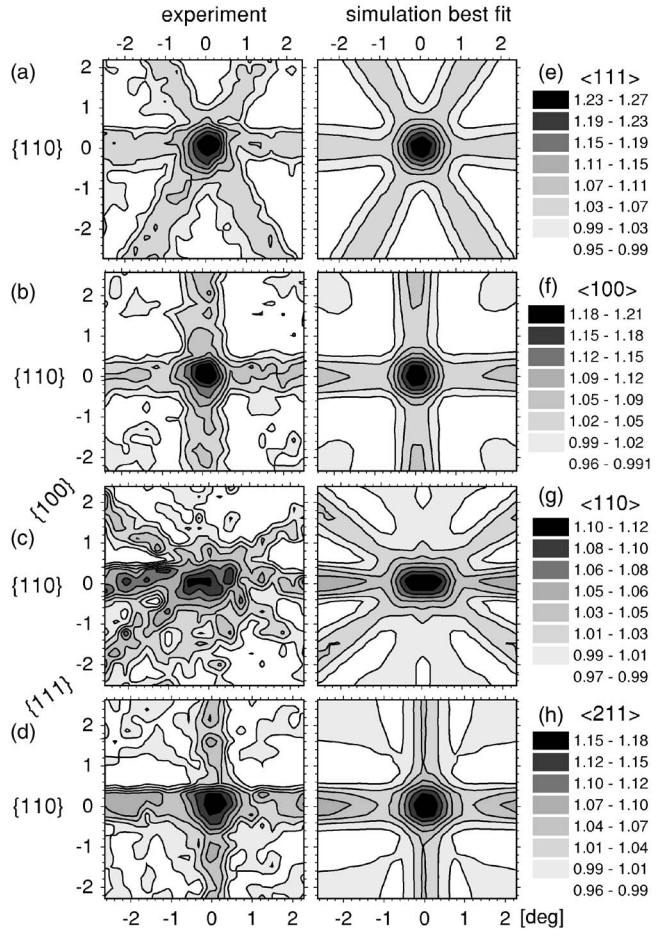

FIG. 1. (a)–(d) Normalized β^- emission yield from sample #8 in the vicinity of ⟨111⟩, ⟨100⟩, ⟨110⟩, and ⟨211⟩ directions following annealing at 300 °C. (e)–(h) Best fit results, corresponding to (e) 5% ($S+T$), 54% near-($S+T$), and 41% R, (f) 12% ($S+T$), 61% near-($S+T$), and 27% R, (g) 3% S, 41% near-S, 22% near-T, and 34% R, (h) 0% S, 39% near-S, 21% near-T, and 40% R.

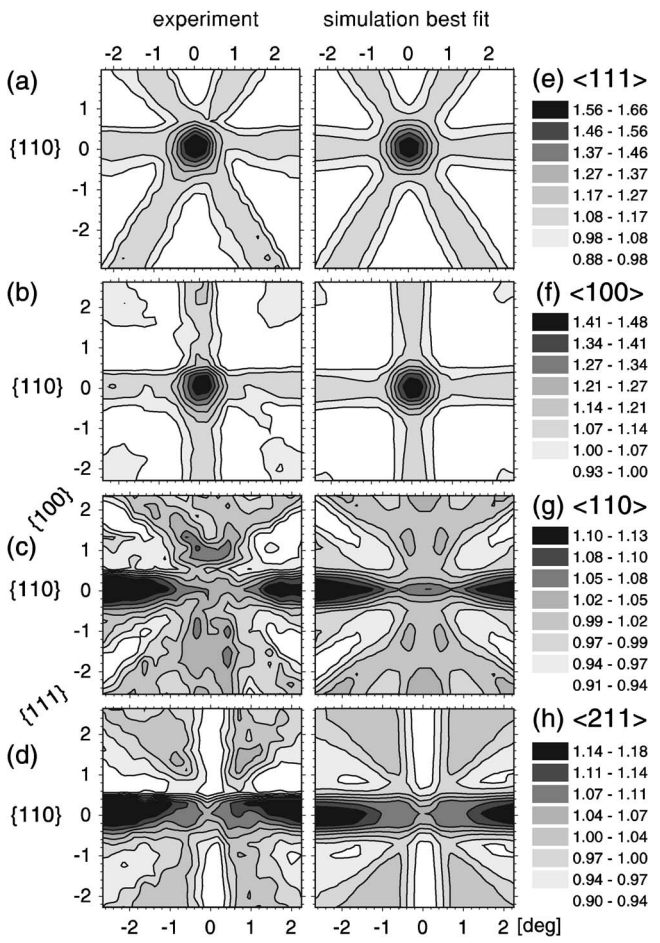

FIG. 2. (a)–(d) Experimental emission channeling patterns from sample #8 following annealing at 600 °C. (e)–(h) Best fit results, corresponding to (e) 30% ($S+T$), 113% near-($S+T$), and −43% R, (f) 30% ($S+T$), 104% near-($S+T$), and −34% R, (g) 11% S, 14% near-S, 75% near-T, and 0% R, (h) 3% S, 34% near-S, 99% near-T, and −36% R.

changed while the maximum anisotropy along these two axes and also along the {110} directions has more than doubled [Figs. 2(a) and 2(b)]. On the other hand, the ⟨110⟩, ⟨211⟩, and {111} effects are now characterized by minima instead of maxima, as is clearly visible in Figs. 2(c) and 2(d). The situation with channeling maxima along ⟨100⟩, ⟨111⟩, and {110} and minima along ⟨110⟩, ⟨211⟩, and {111} is typical for emitter atoms on or close to tetrahedral interstitial (T) positions[36] since the T sites are located within ⟨100⟩ and ⟨111⟩ atomic rows and {110} planes but interstitial with respect to ⟨110⟩, ⟨211⟩, and {111}. Finally, the patterns following 900 °C annealing [Figs. 3(a)–3(d)] are clear proof that the dominant lattice sites of Fe are substitutional again, showing very pronounced channeling along all crystal directions including ⟨110⟩, ⟨211⟩, and {111}.

While the experimental results presented in Figs. 1–3 clearly illustrate changes in the preferred lattice sites of Fe in a qualitative way, quantitative information is obtained from fitting the experimental data by the results of simulations of β^- emission yields for a variety of sites. The general theory for the simulation of emission channeling, the so-called "many beam" approach, is described in Ref. 30 and some computational details on its implementation for Si can be found in Ref. 34. To approximate the continuous β^- energy spectrum of ^{59}Fe, simulations were done for electron energies from 50 keV to 450 keV in steps of 25 keV, and the results averaged according to the theoretical spectral β^- distribution. As one-dimensionally projected root mean square (rms) displacement of Si atoms we used $u_1(\mathrm{Si})=0.0803$ Å, corresponding to a Debye-temperature of 504 K.[37] We calculated characteristic two-dimensional patterns of electron emission probability within a range of ±3° around the ⟨100⟩, ⟨110⟩, ⟨111⟩, and ⟨211⟩ directions in steps of $\Delta x=\Delta y=0.05°$ for S, T, hexagonal interstitial (H), bond center (BC), antibonding (AB), split ⟨100⟩ (SP) and the so-called Y and C sites, as well as ⟨111⟩ and ⟨100⟩ displacements between all of these positions. The location of these sites in the diamond lattice can be found in Refs. 38 and 39. The fit procedures used in order to compare theoretical yields and experimental patterns take into account the angle resolution of the detection setup and have been described in detail previously.[34,35] Note that as a general rule in fitting any emission channeling

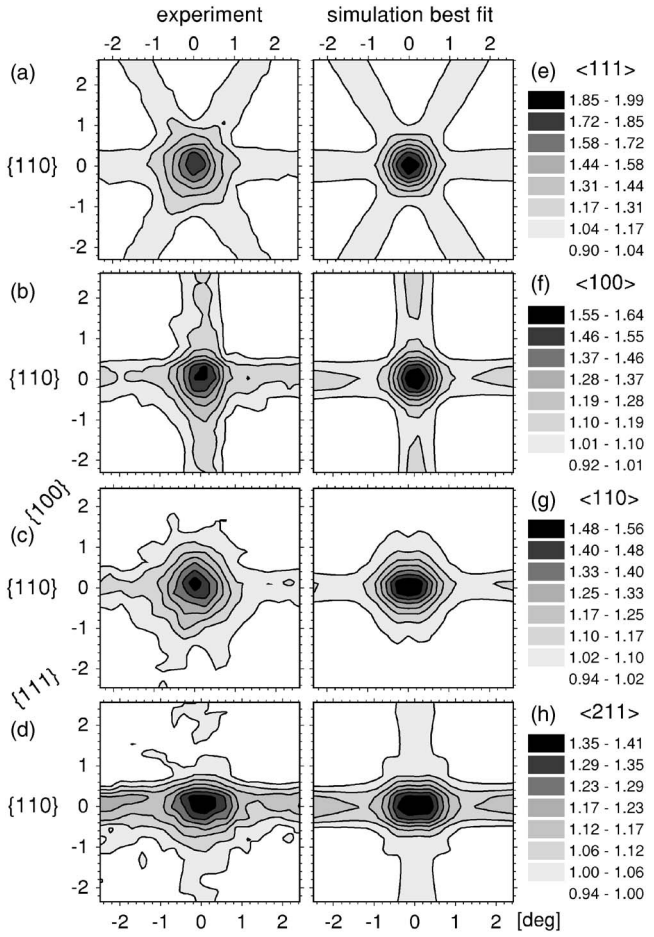

FIG. 3. (a)–(d) Experimental emission channeling patterns from sample #8 following annealing at 800 °C. (e)–(h) Best fit results, corresponding to (e) 29% ($S+T$), 61% near-($S+T$), and 10% (R), (f) 43% ($S+T$), 91% near-($S+T$), and −34% (R), (g) 50% S, 0% near-S, 35% near-T, and 15% (R), (h) 30% S, 10% near-S, and 34% near-T, and 26% (R).

pattern always an isotropic component has to be included, which is given by 1 minus the sum of all other fitted fractions.[30,34,38] Provided that the scattering background and the depth profile of emitter atoms is accurately known and there is no enhanced dechanneling due to defects in the crystal, the isotropic component reflects the fraction of emitter atoms on so-called random (R) sites, which are sites in heavily damaged surroundings or sites of very low crystal symmetry. Consequently, inaccurate knowledge of the scattering background or emitter depth profile will lead to inaccuracies in assessing the fraction of emitter atoms on R sites.

It turned out that our experimental results can only be satisfactorily described by, apart from Fe on random sites, considering Fe on at least three distinct lattice sites: ideal substitutional sites, displaced substitutional sites, and displaced tetrahedral interstitial sites. While the samples always contain a mixture of Fe on these three lattice sites and random sites, Fe on near-S sites dominates the patterns in the as-implanted state and following annealing up to 300 °C (Fig. 1). On the other hand, Fe on near-tetrahedral interstitial sites is best visible following annealing at 600 °C (Fig. 2),

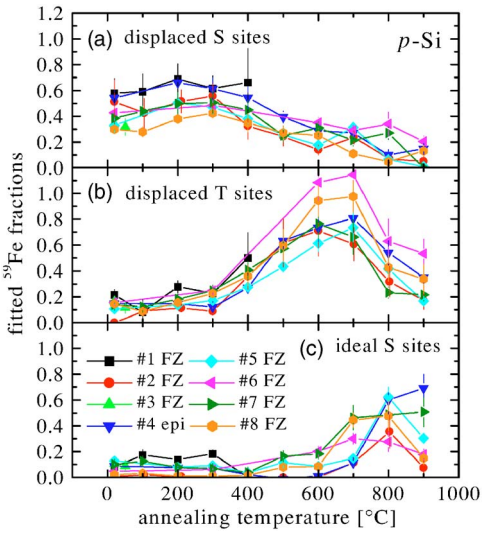

FIG. 4. (Color online) Fractions of ^{59}Fe on the three different lattice sites for the p-type samples #1–8, derived from fits to the experimental patterns assuming an as-implanted depth profile of ^{59}Fe. Sample #3 was only annealed up to 50 °C and sample #1 only up to 400 °C.

and Fe on ideal S sites following annealing at 800–900 °C (Fig. 3). By ideal substitutional sites we mean Fe on substitutional sites showing isotropic Gaussian displacements with $u_1=0.079$ Å due to thermal vibrations only. The value of 0.079 Å is a best guess assuming that Fe acts as a simple mass defect in the Si lattice. The displaced substitutional sites are sites exhibiting static displacements around 0.4–0.7 Å from the ideal S position, and the displaced tetrahedral interstitial sites are located 0.3–0.8 Å from the ideal T position. Both in case of the near-S and near-T sites all possible displacements from the ideal S and T sites along ⟨111⟩ and ⟨100⟩ directions were tried in the fits. However, similar chi square values were obtained and the direction of the static displacement could therefore not be pinpointed. The values of 0.4–0.7 Å and 0.3–0.8 Å for the displacements thus represent the statistical uncertainty, taking into account displacements along different crystal directions that lead to a similar quality of fit. The best fit results to the experimental patterns obtained are shown in Figs. 1–3 panels (e)–(h). Note that we cannot exclude that additional lattice sites play a certain minor role, especially ideal T sites could be occupied to some smaller extent as well.

Figures 4 and 5 show the best fit fractions for the three considered sites as a function of annealing temperature for the p-type and n-type samples, respectively. We first note that all samples showed the general feature of site changes from near-S to near-T and then to S with increasing annealing temperature. Second, within the range of doping types studied (all samples were relatively moderately doped), there are no significant differences visible between n- and p-type Si. Also no clear trend distinguishes the results obtained with oxygen-lean float-zone (FZ) or oxygen-rich Czochralski (CZ) material, and even the implanted fluence, which ranged from 1.4×10^{12} cm^{-2} to 1.0×10^{14} cm^{-2}, seems to have no pronounced effect on the lattice location of Fe. Third, we note that for annealing temperatures at 600 °C and above the

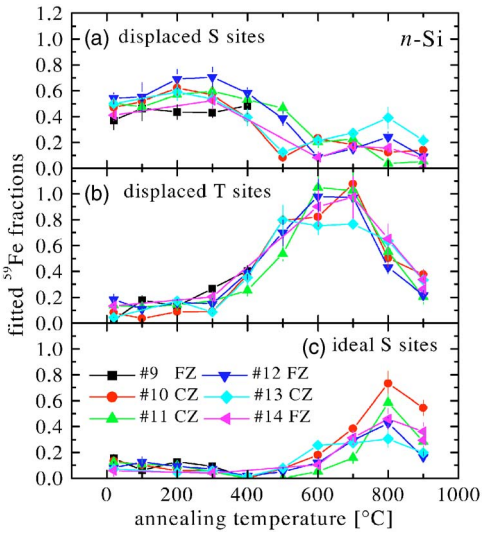

FIG. 5. (Color online) Fractions of ^{59}Fe on the three different lattice sites for the *n*-type samples #9–14, derived from fits to the experimental patterns assuming an as-implanted depth profile of ^{59}Fe. Sample #9 was only annealed up to 400 °C.

sum of the three fitted fractions generally becomes larger than 100% and the random fraction (not shown) reaches negative values. An explanation for this apparently unphysical result will be given below.

IV. DISCUSSION

In interpreting the results of our lattice location experiments one has to consider the damage created during the ion implantation process. It is estimated from SRIM (Ref. 32) or MARLOWE simulations[33] that around 800–1300 vacancies and interstitials are created for every implanted Fe atom. The simulations indicate that the initial vacancy distribution is approximately a Gaussian of 330 (295) Å, i.e., centered at somewhat more than half of the projected range of the implants. However, it is clear that annealing considerably changes the concentration and nature of the vacancy-like defects, with simple vacancies annihilating with interstitials or clustering into multiple vacancies. Fe obviously reacts with some of the vacancy-like defects, which leads to its incorporation on or near substitutional sites, similar to the case of Cu in Si, which we investigated previously.[39–41]

However, while there exist some parallels between our current results on Fe in Si and our previous findings on the lattice location of implanted Cu in Si, there are also significant differences. Both of the implanted transition metals were found mostly on near-substitutional sites in the room-temperature as-implanted state. In the case of Cu, annealing above 200 °C resulted in Cu progressively disappearing from near-substitutional sites and being incorporated on random sites. Assuming a simple one-step model for this process, we estimated an activation energy around 2.2 eV for the dissociation of near-substitutional Cu, and if retrapping at vacancies from the implantation process was included in the model, the estimate was somewhat lower, around 1.8 eV.[40,41] Fe also starts to disappear from near-substitutional sites at similar annealing temperatures, and its stability at near-substitutional sites can therefore be estimated to be also around 2.0 eV. However, instead of escaping to random sites it is increasingly found on displaced-tetrahedral interstitial sites following annealing at temperatures between 400 °C and 700 °C. Cu is an ultrafast diffuser in Si, which means it easily reacts with other defects even at room temperature and its interstitial state is hence extremely difficult to observe. On the other hand, it is well known that Fe can be quenched in the interstitial state following high-temperature annealing.[2,3,9] Although all our samples were cooled slowly it might therefore be that the pronounced interstitial fraction of Fe simply represents quenched interstitial Fe which remains after the near-substitutional Fe complexes have broken up, interstitial Fe has been diffusing a short distance in the sample and the sample is cooled to room temperature again. What is not in favor of this interpretation, however, is the fact that the interstitial Fe is clearly displaced around 0.3–0.8 Å from the ideal *T* position. As will be discussed below in conjunction with Mössbauer results from the literature, it seems possible that the near-*T* Fe is due to Fe_i-*V* complexes, i.e. interstitial Fe bound to a neighboring vacancy.

With respect to transition metals on ideal substitutional sites, we have previously observed the incorporation of Cu on ideal *S* sites, however, only in highly *n*-type Si and following annealing between 500 °C and 700 °C.[41] Fe on ideal *S* sites is clearly observed in moderately doped *n*- and *p*-Si and its stability is significant since it is still present in considerable amounts in many samples even following annealing at 900 °C.

We should note here that the damage created during implantation exceeds the *n*- or *p*-doping level of all our samples by orders of magnitude. For instance, the electrically active *P* concentration in the sample with lowest resistivity (sample #11) corresponds to roughly 1.7×10^{17} cm^{-3}. Even in the sample implanted with lowest fluence (sample 1 with 1.4×10^{12} cm^{-2}) the concentration of Fe reaches 1.4×10^{17} cm^{-3} in the peak of the implantation profile, and the initial defect concentration is even around three orders of magnitude higher. It is hence likely that the Fermi level is in midgap position in the implanted region, which would explain why we did not observe major differences between moderately doped *n*- and *p*-type Si. Samples with much higher doping levels (n^+ or p^+ material) have to be used in order to investigate a possible influence of the Fermi level on the lattice location of Fe. Such measurements are currently under way, and preliminary results show that the interstitial fraction of Fe is dominant in p^+-Si while it is considerably reduced in n^+-Si.

We will now discuss the fact that the fitted fractions of Fe reaches values above 100%. Since dechanneling due to the thermal motion of the Si atoms causes an approximately exponential damping of the wave function of channeled electrons, the intensity of the channeling effects depends on the depth profile of the emitter atoms. In our analysis we have assumed Gaussian ^{59}Fe depth profiles of 532(192) Å resulting from 60 keV implantation. However, it has been reported[42] that Fe implanted to a fluence of 1×10^{15} cm^{-2} in Si is pushed towards the surface during solid phase epitaxial

regrowth. Following implantation of Si samples with various heavy ions it was also observed that Fe and other transition metals such as Cu preferentially decorate two regions in the implanted sample: the end of range of the implanted ions, the so-called *Rp*-region, and midway between the projected range and the surface, the so-called *Rp*/2-region.[4–8] It has been suggested that vacancy-type defects at half of the projected range act as effective gettering sites for Fe in the *Rp*/2 region.[8] We have therefore also undertaken simulations for shallower depth profiles of Fe, centered at half of the 60 keV implantation depth. Under these assumptions the sum of the regular Fe fractions would be around 80%. Redistribution of the Fe towards the crystal surface and the resulting badly defined emitter depth profiles could thus well explain the apparent fractions larger than 100% and also the considerable differences in fractions between various samples.

It is well known that Fe in Si tends to form thermodynamically stable silicide precipitates.[1–4] Hence one might expect that the lattice sites following high-temperature annealing represent Fe within small silicide precipitates and the formation of the precipitates to depend on the Fe concentration of the samples. It is therefore very surprising that no correlation of the various Fe lattice sites with the implanted fluence was observed. This puzzling behavior will need to be investigated in further experiments using higher implanted doses of Fe.

V. COMPARISON WITH MÖSSBAUER AND EPR DATA

Our observation of Fe on ideal *S*, near-*S*, and near-*T* sites also gives valuable information for the interpretation of Mössbauer spectroscopy (MS) and EPR experiments. We generally confirm the existence of interstitial Fe and substitutional Fe as inferred from MS, however, a 1:1 correspondence between channeling and MS results is complicated by the fact that most of the available Mössbauer data rely on completely different annealing time scales than emission channeling and many other techniques. Basically all MS results at low Fe concentrations were observed in source experiments either following Coulomb excitation of ^{57}Fe (Ref. 17, 20, and 26) or following the implantation and decay of ^{57}Mn ($t_{1/2}$=1.7 min).[21–27] In Coulomb excitation experiments (which we will abbreviate as ^{57}Fe*) a large recoil always accompanies the heavy ion bombardment excitation process, and in ^{57}Mn$\rightarrow$^{57}Fe decay experiments a $\sim$40 eV recoil results from the nuclear decay of ^{57}Mn. Therefore, in both cases the MS level probes the situation in a narrow time window ($\sim$140 ns) immediately after recoil implantation. While any reaction of Fe *itself* can only be studied on this time scale, the overall damage accumulation and damage annealing in the sample is dominated by the fact that the experiments are done on-line, i.e. the measurement temperature is also the implantation temperature. Due to dynamic annealing, implantations at elevated temperatures result in considerably reduced concentrations of primary defects while secondary defect complexes become more prominent. In addition, the outcome of the experiment may depend on the thermal history of the sample, e.g., if the experiment is started at low temperatures, initially defects are accumulating in the sample which are then annealed during subsequent implantations at higher temperature. Thermally activated reactions hence take place on two or three different time scales: (1) the time window due to the 140 ns lifetime of the MS level in ^{57}Fe, (2) the time scale of changing to and measuring at a certain implantation temperature, and (3) in case of ^{57}Mn$\rightarrow$^{57}Fe experiments also the 1.7 min half life of ^{57}Mn during which the Mn atom can react with other defects present in the sample.

The on-line MS experiments have clearly shown that at low temperatures the recoil implantation results in high fractions of the singlet interstitial centers (b) (30%–50%) and the damage doublet (a) (50%–70%). The damage doublet (a) disappears to a large extent already below room temperature and is undetectable above 200 °C.[21,23–25] In ^{57}Mn$\rightarrow$^{57}Fe experiments the intensity of the singlet substitutional center (c) continuously increases above 100 K and finally remains constant only above 180 °C,[23–25] while in ^{57}Fe* studies it only appears above $\sim$350 °C.[17,20] This difference in temperature may be due to the fact that in ^{57}Fe* experiments these centers can definitely only be formed during the 140 ns lifetime, while in ^{57}Mn$\rightarrow$^{57}Fe studies they may be formed already by the ^{57}Mn precursor and survive its decay. In ^{57}Mn$\rightarrow$^{57}Fe experiments above 100 °C the "new line" (d) starts to appear which persists even at 500 °C.[23,24] The low Debye temperature of this "new line" points to interstitial Fe and it has been suggested to be due to Fe$_i$-V complexes where Fe sits 0.4 Å from the ideal *T* site, and, moreover, to be identical to the *NL*19 center observed by EPR.[23,24]

A similar recoil (200 eV) as in the MS experiments is received by the ^{59}Fe in our case when the ^{59}Mn nucleus decays a few seconds after its implantation into the Si sample. However, our channeling measurements cannot probe the situation immediately following the ^{59}Mn decay and the resulting ^{59}Fe recoil implantation. On the contrary, the samples were typically stored at least several hours, in some cases days or weeks, at room temperature before the first measurements were started, thus giving enough time for interstitial Fe to react with vacancies, which obviously resulted in the majority of Fe occupying the near-*S* sites and most of the rest random sites. As was already mentioned, we cannot exclude small fractions (10%–15%) of Fe on ideal tetrahedral interstitial sites in our experiments but they are certainly not the dominating interstitial sites responsible for the patterns shown in Fig. 2. It seems possible that ideal *T* sites might be occupied only immediately after implantation well below room temperature, or, as was done for the EPR identification of Fe$_i^+$ or Fe$_i^0$,[1,2,9] following a fast quench of Fe-containing Si from temperatures near its melting point.

Assuming that a similar scenario of site changes from near-*S* to near-*T* to ideal *S* also occurs in on-line MS experiments but taking into account that annealing temperatures do not need to correspond to those in emission channeling or EPR experiments, we propose the correspondence between emission channeling, MS and EPR data shown in Table II. The identification of the *NL*19 EPR center with near-*S* or near-*T* sites is based on the suggestion that this center consists of a Fe-vacancy complex of trigonal symmetry,[18,19] a microscopic model which would fit both near-*S* or near-*T* Fe. However, the reported annealing temperatures of the *NL*19

TABLE II. Proposed correspondence between the Fe lattice sites found in emission channeling experiments, the lines identified in Mössbauer studies, and major EPR centers.

Emission channeling	Mössbauer	EPR
Random	(a) damage doublet	
Ideal *T* interstitial (not seen)	(b) interstitial singlet	Fe_i^+ and Fe_i^0
Near-*S*	(c) substitutional singlet	*NL*19
Near-*T* interstitial	(d) interstitial "new line" doublet	*NL*19 ?
Ideal *S*	either not yet seen or (c) substitutional singlet	not seen

center, which scatter from 160 °C (Ref. 18) to 500 °C (Ref. 19), rather point to Fe on near-*S* sites. Our experiments show that the incorporation of large fractions of Fe on ideal substitutional sites requires annealing temperatures above 700 °C. Since these temperatures have not been reached in on-line Mössbauer experiments, it seems possible that they did not produce Fe on ideal *S* sites in sufficient quantitities to be detected.

VI. CONCLUDING REMARKS

Our study confirmed that Fe in Si exhibits a richness of structural properties, in particular that it is able to occupy at least three different lattice sites: near-tetrahedral interstitial sites, near-substitutional sites, and ideal substitutional sites. We provided the first direct evidence for Fe on or near-substitutional sites in Si, thus confirming the interpretation of Mössbauer data. The fact that at least three different Fe sites were clearly observed shows the demand for a more refined theoretical treatment of the structural properties of Fe-related defects in Si.

Finally, our results, which are consistent with implanted Fe being trapped by vacancy like defects at the end of its projected range and, following annealing above 600 °C, also around half of its implanted range, provided further insight in the nature of the defects responsible for the gettering behavior of radiation damage.

ACKNOWLEDGMENTS

We would like to thank G. Weyer for helpful discussions and comments on the manuscript. This work was funded by the Portuguese Foundation for Science and Technology (FCT), Project No. CERN/FIS/43725/2001. The ISOLDE beam times were supported by the European Commission (Large Scale Facility Contract No. HPRI-CT-1999-00018). U. Wahl and E. Rita acknowledge support by the FCT, Portugal.

*Corresponding author. Electronic address: uwahl@itn.pt

[1] E. R. Weber, Appl. Phys. A: Solids Surf. **30**, 1 (1983).
[2] A. A. Istratov, H. Hieslmaier, and E. R. Weber, Appl. Phys. A: Mater. Sci. Process. **69**, 13 (1999).
[3] A. A. Istratov, H. Hieslmaier, and E. R. Weber, Appl. Phys. A: Mater. Sci. Process. **70**, 489 (2000).
[4] S. M. Myers, M. Seibt, and W. Schröter, J. Appl. Phys. **88**, 3795 (2000).
[5] R. A. Brown, O. Kononchuk, G. A. Rozgonyi, S. Koveshnikov, A. P. Knights, P. J. Simpson, and F. González, J. Appl. Phys. **84**, 2459 (1998).
[6] S. V. Koveshnikov and G. A. Rozgonyi, J. Appl. Phys. **84**, 3078 (1998).
[7] R. Kögler, R. A. Yankov, J. R. Kaschny, M. Posselt, A. B. Danilin, and W. Skorupa, Nucl. Instrum. Methods Phys. Res. B **142**, 493 (1998).
[8] R. Krause-Rehberg, F. Börner, F. Redmann, J. Gebauer, R. Kögler, R. Kliemann, W. Skorupa, W. Egger, G. Kögel, and W. Triftshäuser, Physica B **308**, 442 (2001).
[9] G. W. Ludwig and H. H. Woodbury, Solid State Phys. **13**, 223 (1962).
[10] A. Zunger and U. Lindefelt, Phys. Rev. B **26**, 5989 (1982).
[11] U. Lindefelt and A. Zunger, Phys. Rev. B **30**, 1102 (1984).
[12] H. Katayama-Yoshida and A. Zunger, Phys. Rev. B **31**, 7877 (1985).
[13] F. Beeler, O. K. Andersen, and M. Scheffler, Phys. Rev. B **41**, 1603 (1990).
[14] H. Weihrich and H. Overhof, Phys. Rev. B **54**, 4680 (1996).
[15] H. Overhof and H. Weihrich, Phys. Rev. B **55**, 10508 (1997).
[16] A. Zunger and U. Lindefelt, Phys. Rev. B **27**, 1191 (1983).
[17] J. Kübler, A. E. Kumm, H. Overhof, P. Schwalbach, M. Hartick, E. Kankeleit, B. Keck, L. Wende, and R. Sielemann, Z. Phys. B: Condens. Matter **92**, 155 (1993).
[18] S. H. Muller, G. M. Tuynman, E. G. Sieverts, and C. A. J. Ammerlaan, Phys. Rev. B **25**, 25 (1982).
[19] T. Mchedlidze and M. Suezawa, Jpn. J. Appl. Phys., Part 1 **41**, 7288 (2002).
[20] P. Schwalbach, S. Laubach, M. Hartick, E. Kankeleit, B. Keck, M. Menningen, and R. Sielemann, Phys. Rev. Lett. **64**, 1274 (1990).
[21] G. Weyer, A. Burchard, M. Fanciulli, V. N. Fedoseyev, H. P. Gunnlaugsson, V. I. Mishin, R. Sielemann, and the ISOLDE collaboration, Physica B **273**, 363 (1999).
[22] H. P. Gunnlaugsson, G. Weyer, M. Dietrich, M. Fanciulli, K. Bharuth-Ram, and R. Sielemann, Appl. Phys. Lett. **80**, 2657 (2002).
[23] H. P. Gunnlaugsson, M. Fanciulli, M. Dietrich, K. Bharuth-Ram, R. Sielemann, and G. Weyer, Nucl. Instrum. Methods Phys. Res. B **186**, 55 (2002).
[24] H. P. Gunnlaugsson, G. Weyer, N. E. Christensen, M. Dietrich, M. Fanciulli, K. Bharuth-Ram, R. Sielemann, and the ISOLDE collaboration, Physica B **340**, 532 (2003).
[25] G. Weyer, H. P. Gunnlaugsson, M. Dietrich, M. Fanciulli, R. Sielemann, and the ISOLDE collaboration, Nucl. Instrum. Meth-

ods Phys. Res. B **206**, 90 (2003).
[26] G. Langouche, Hyperfine Interact. **72**, 217 (1992).
[27] Y. Kobayashi, Y. Yoshida, M. K. Kubo, Y. Yamada, A. Yoshida, H. Ogawa, H. Ueno, and K. Asahi, Eur. Phys. J. A **13**, 243 (2002).
[28] B. A. Bunker, J. Vac. Sci. Technol. A **5**, 3003 (1987).
[29] I. A. Vartanyantz, J. Auleytner, L. Nowicki, S. Kwiatkowski, and A. Turos, Acta Phys. Pol. A **89**, 625 (1996).
[30] H. Hofsäss and G. Lindner, Phys. Rep. **210**, 121 (1991).
[31] V. N. Fedoseyev, K. Bätzner, R. Catherall, A. H. M. Evensen, D. Forkel-Wirth, O. C. Jonsson, E. Kugler, J. Lettry, V. I. Mishin, H. L. Ravn, G. Weyer, and the ISOLDE collaboration, Nucl. Instrum. Methods Phys. Res. B **126**, 88 (1997).
[32] J. F. Ziegler, Nucl. Instrum. Methods Phys. Res. B **219**, 1027 (2004).
[33] M. T. Robinson, Phys. Rev. B **40**, 10717 (1989).
[34] U. Wahl, Hyperfine Interact. **129**, 349 (2000).
[35] U. Wahl, J. G. Correia, A. Czermak, S. G. Jahn, P. Jalocha, J. G. Marques, A. Rudge, F. Schopper, J. C. Soares, A. Vantomme, P. Weilhammer, and the ISOLDE collaboration, Nucl. Instrum. Methods Phys. Res. A **524**, 245 (2004).
[36] U. Wahl, A. Vantomme, J. De Wachter, R. Moons, G. Langouche, J. G. Marques, J. G. Correia, and the ISOLDE collaboration, Phys. Rev. Lett. **79**, 2069 (1997).
[37] L. V. Hau, E. Laegsgaard, and J. U. Andersen, Nucl. Instrum. Methods Phys. Res. B **48**, 244 (1990).
[38] U. Wahl and the ISOLDE collaboration, Phys. Rep. **280**, 145 (1997).
[39] U. Wahl, J. G. Correia, A. Vantomme, G. Langouche, and the ISOLDE collaboration, Physica B **273**, 367 (1999).
[40] U. Wahl, A. Vantomme, G. Langouche, J. G. Correia, and the ISOLDE collaboration, Phys. Rev. Lett. **84**, 1495 (2000).
[41] U. Wahl, A. Vantomme, G. Langouche, J. P. Araújo, L. Peralta, J. G. Correia, and the ISOLDE collaboration, Appl. Phys. Lett. **77**, 2142 (2000).
[42] J. P. de Souza, L. Amaral, and P. F. P. Fichtner, J. Appl. Phys. **71**, 5423 (1992).